Towards Uncertainty Analysis of CFD Simulation of Ship Responses in Regular Head Waves

Towards Uncertainty Analysis of CFD Simulation of Ship Responses in Regular Head Waves

Mohsen Irannezhad[1,*], Rickard E. Bensow[1], Martin Kjellberg[2], and Arash Eslamdoost[1]

[1]Chalmers University of Technology, 412 96, Gothenburg, Sweden
[2]SSPA Sweden AB, 412 58, Gothenburg, Sweden
[*]Corresponding author, E-mail: mohsen.irannezhad@chalmers.se

INTRODUCTION

Ship hydrodynamic performance prediction in waves is a common practice in the early stages of the ship design process as the interaction between the ship and waves may adversely affect the hydrodynamic responses of the ship in comparison to calm water. Various well-established numerical and experimental methods are often utilized for prediction of ship performance in waves. Although the model tests are expensive and time-consuming, a high level of accuracy is often achieved in such experiments. On the other hand, with respect to the increased computational power, prediction of ship performance in waves by the numerical methods based on Computational Fluid Dynamics (CFD) techniques are gradually acquiring more popularity. However, the validity of the incorporated discretization schemes and modelling assumptions in these state-of-the-art CFD methods are often overlooked and the method accuracy is mainly assessed through the validation of the results based on the respective model test data. Validation as an engineering exercise aims to show that the right equations are solved, while verification (mathematical exercise) is required to demonstrate that equations are solved right [1].

The eventual objective of this research is to perform verification and validation exercises of a ship performance prediction in regular head waves using CFD, whereas in this paper, the working progress is presented which may be subjected to significant revisions. To this end, extensive attempts have been made to investigate numerical wave propagation without the presence of the hull. Ship responses in waves are significantly influenced by the wave excitation forces. Therefore, not only high level of accuracy is required for the simulation of the numerical waves, but also quantification of the numerical uncertainties are of a great importance. This becomes even more challenging when the ship hydrodynamic responses, such as motions and added resistance in waves, exhibit dependencies on wave steepness. In this paper, the main focus of such uncertainty analyses is on the systematic grid convergence study.

APPROACH

The second variant of the MOERI tanker (KVLCC2) in model-scale (scale factor = 100) and operating in fresh water at the design speed (Froude number $Fr = 0.142$) in a regular head wave (wave height $H = 0.06\ m$ and wave length $\lambda/L = 0.6$) is considered. The model tests are carried out in Osaka University Towing Tank [2].

In this paper, a commercial CFD solver, Simcenter STAR-CCM+ (version 2020.3.1), is used with an Unsteady Reynolds-Averaged Navier-Stokes (URANS) approach. Unstructured grids including the trimmed hexahedral meshes with local refinements near the free surface and near the hull as well as prism layer meshes along the hull surface are generated using STAR-CCM+ automatic mesh generator. Different cautions are taken into account to eliminate/diminish undesired grid refinement diffusion depths (transition zone between two local refinement zones) and also to generate ”as geometrically similar as possible” set of unstructured grids. The computational domain in each grid is discretized employing an Overset Topology which consists a moving overset region and a stationary background region with specific treatment of cell sizes near the overlapping zone (where the information is exchanged between the background and overset regions).

The simulations are mainly carried out for five different grid sets shown in Table 1, in which the effects of different local refinement zones as well as the quality of the cell size and overset interpolations in the overlapping zones are evaluated. The simulations are carried out in three different computational domain widths, i.e., Quasi-2D (only one cell in Y direction), Small Width SW-3D (one third of the full domain in Y) and Full Width FW-3D (full domain size in Y). The reason behind choosing one third of the domain size for the SW-3D case is to eliminate undesired grid refinement diffusion depths that may be introduced by the grid generator. In GS4, a sinusoidal pitch

motion with an amplitude of 3 (deg) and a frequency equal to the wave encounter frequency is predefined for the overset region.

Table 1: Grid sets details.

Grid Set	Simulation Type	Regions		Local Refinement Zones					Prism Layers
		Background	Overset	Free Surface	Kelvin Wedge	Overlapping	Around Overset	Inside Overset	
GS1	Wave Propagation	✓	–	✓	–	–	–	–	–
GS2	Wave Propagation	✓	–	✓	✓	✓	✓	–	–
GS3	Wave Propagation	✓	✓ Restrained	✓	✓	✓	✓	✓	–
GS4	Wave Propagation	✓	✓ Predefined Motions	✓	✓	✓	✓	✓	–
GS5	Hull Performance	✓	✓ Hull Motions	✓	✓	✓	✓	✓	✓

In each grid set, four systematically refined grids are considered which are determined by the refinement levels $n = 0.5$ (coarsest), 1.0, 1.5 and 2.0 (finest). Trimmed hexahedral meshes (isotropic volume meshes) are generated in both background and overset regions, where every two cells are divided into $2n$ cells in each direction (except in Y for Quasi-2D simulations) to derive a geometrically similar grids. Figure 1 shows the grids ($n = 1.0$ and 1.5) in GS2 where different local refinement zones are illustrated by different colors. The total number of cells in SW-3D domain in each grid in GS1, GS2 and GS3 (equal to GS4) is exactly 984384, 4122656 and 6606944 multiplied by n^3, respectively.

In order to achieve geometrically similar anisotropic sub-layer (prism layer) meshes, the methodology presented by P. Crepier [3] is employed. In this method, the total thickness of prism layers remains the same between the grids but both the first layer cell thickness and the growth ratio between the layers are adjusted accordingly. The total number of layers in each grid will be nN_t, in which N_t is the total number of layers for the coarsest grid, see Figure 2. The prism layers are generated such that the non-dimensional wall distance y^+ remains above 30 over the major part of the hull wetted surface area during the ship simulations in waves (for all grids in GS5), hence a wall function is utilized for treatment of the near-wall region. The undesired transition zone between the prism layers and their neighbouring isotropic cells are inevitable in GS5, consequently, the total number of cells are 987823, 7868343, 26542331 and 62866494 for $n = 0.5 - 2.0$, respectively.

An overview of the computational domain size and the imposed boundary conditions are shown in Figure 3. Moreover, 16 wave probes (located at 4 X-positions and 4 Y-positions) are considered in order to analyze the numerical wave elevation. The longitudinal location of probes are, (1) at the end of wave forcing zone (will be explained further in the paper), (2) before the overset region, (3) within the overlapping zone and, (4) inside the overset region close to the hull fore perpendicular. Notice that the hull was not present in the wave propagation simulations in GS1-GS4. Although the Quasi-2D simulations are computationally much cheaper than 3D simulations, it was found that the Quasi-2D results for the wave propagation simulations are not necessarily similar to that of the 3D cases. Therefore, the wave propagation simulations are mainly performed in SW-3D domain in order to gain similar results as of FW-3D while keeping the computational costs low. Thereafter, the hull performance simulations are carried out only in the FW-3D domain.

The Volume of Fluid (VOF) model is used to capture the free surface. A wave forcing function is used in the vicinity (distance equal to L) of all vertical boundaries with velocity inlet boundary conditions in order to force the solution of the discretized Navier-Stokes equations towards the theoretical 5^{th} order Stokes wave solution minimizing the wave reflection from the boundaries. An implicit unsteady solver is used with a second order temporal discretizational scheme (time step $t = 0.003/n$, hence similar Courant number between the grids in each grid set). The chosen time step results in Courant numbers smaller than 0.3-0.4 on the free surface which also fulfils the ITTC recommendations of at least 100 time steps per encountered wave period [4].

In the wave propagation simulations, both the background and overset regions are moved with a constant speed translation motion representing the hull expected velocity. On the other hand, in the experimental model tests, the hull was towed with a light weight carriage connected to the main carriage by means of a weak spring in order to allow the ship to surge in conjunction with heave and pitch. This weak spring mass system is also numerically replicated in the simulations, therefore the hull actual velocity and hence the translation motion of the background and overset regions in the hull performance simulations is marginally oscillate around the hull

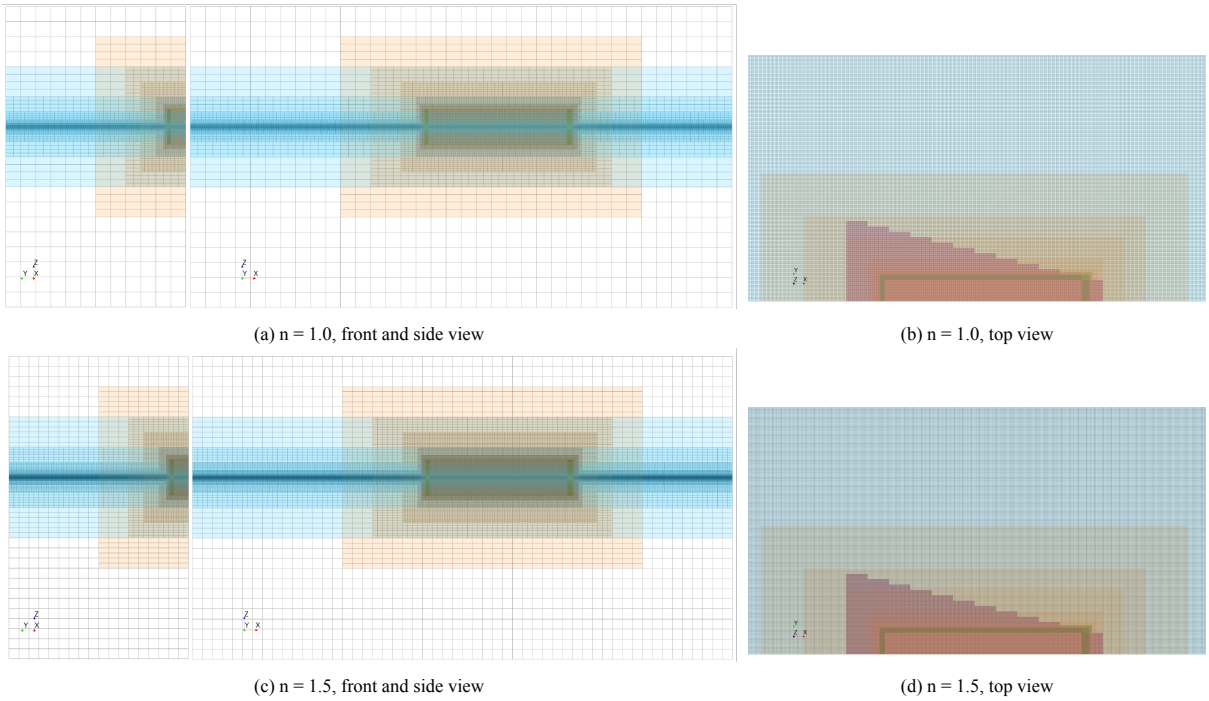

(a) n = 1.0, front and side view

(b) n = 1.0, top view

(c) n = 1.5, front and side view

(d) n = 1.5, top view

Figure 1: Overview of the grids and local refinement zones (Free Surface Around Overset Overlapping Kelvin Wedge) for GS2 in FW-3D domain.

expected velocity.

RESULTS

The numerical wave elevation ζ and its error (relative to the analytical representation of the 5th order Stokes wave) after 30 encountered waves are presented for GS1 (in SW-3D domain) in Figure 4a. Moreover, the longitudinally averaged absolute error (in percentage of the wave height) for Laminar and Turbulent flow (k-ω SST) simulations are presented in Figure 4b. The results of the turbulent flow simulations are similar to that of laminar flow. Wave propagation is a laminar phenomenon by its nature, while turbulent simulations are required when the hull performance is being studied.

The averaged absolute error is rather low for both laminar and turbulent flow simulations in GS1. Moreover, the error converges approximately after a few encountered wave periods. Therefore, the simulations deemed converged after 12 encountered waves and the Fourier analysis of the wave elevation at the probes are carried out for GS1-GS4 over the 12-20 encountered wave periods time window. The 1^{st} harmonic amplitude as the domi-

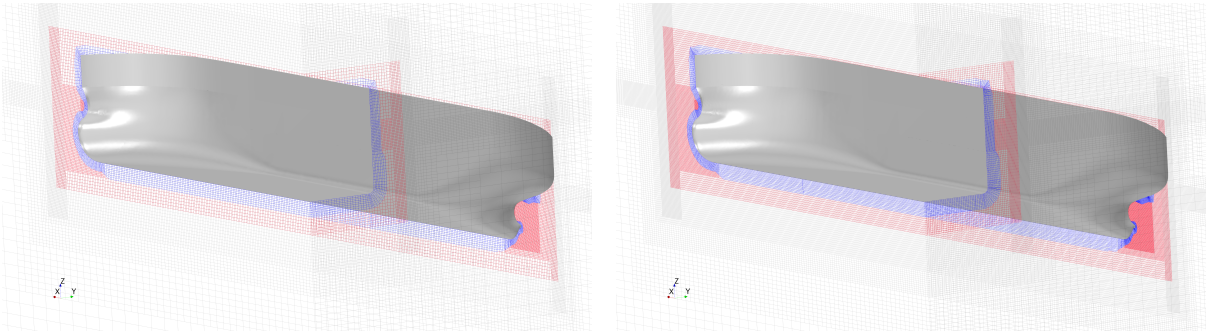

(a) n = 1.0

(b) n = 1.5

Figure 2: Overview of the grids near the hull in GS5. Gray lines represents the mesh in the background region. Blue and red colors represent the isotropic and prism layer meshes in the overset region, respectively. Local refinement zones inside the overset can also be observed.

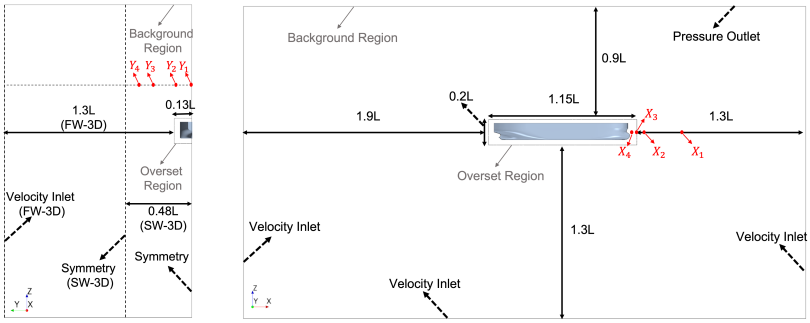

Figure 3: Computational domain size, applied boundary conditions and wave probes locations.

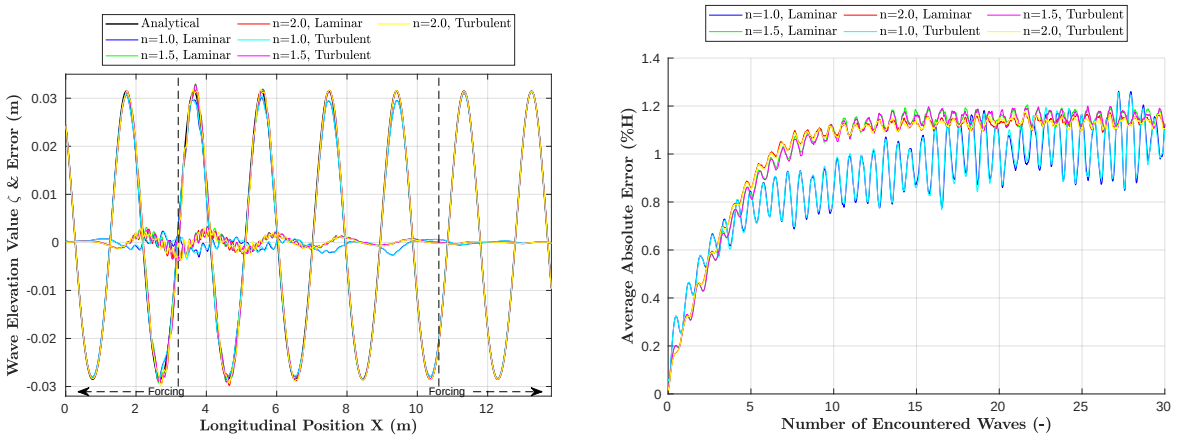

(a) Wave elevation after 30 encountered periods

(b) Monitored averaged absolute error

Figure 4: Wave elevation near symmetry plane (Y_1) and its error with respect to the analytical wave elevation for GS1 in SW-3D domain.

nating component is shown in Figure 5. It should be noted that the magnitudes of the higher harmonic components are very small, thereby small differences yield large errors.

It can be clearly seen that for all the grid sets and all the probes, the magnitude of the error for $n = 0.5$ is considerably larger than the finer grids. For X_1 probes (located at the end of forcing zone), shown in Figure 5a, the magnitudes of errors decrease from coarsest to finer grids in all grid sets. Moreover, the results for different grid sets and an specific refinement level are very similar, hence no significant effects from the local refinements and overset region at that longitudinal location are observed. The results are also similar for different Y probes in each refinement level.

For X_2 probes (before the overset region), shown in Figure 5b, the magnitude of error for GS1 decreases from coarser grids towards finer grids, while for GS2, GS3 and GS4 the behaviour varies depending on the grid refinement and the probes Y location. On the other hand, the magnitude of the error is relatively smaller for $n = 1.5, 2.0$ compared to the coarser grids. Interestingly, for GS4 in all refinement levels for Y_1 and Y_2 (located closer to the pitching overset region) the change of error is towards positive values which results in decreased error in $n = 0.5, 1.0$ and increased error in $n = 1.5, 2.0$ (although negligible).

For X_3 probes (only Y_1 and Y_2 are located within the overlapping zone for the grid sets including overlapping refinement), shown in Figure 5c, almost similar trend as of X_2 probes is seen, however, with a more pronounced change of errors in Y_1 and Y_2 for GS4. This may imply that the overset interpolations are affected more significantly in the case of the existing pitch motion than the restrained overset region in GS3. For probes located at X_4 (only Y_1 and Y_2 are located inside the overset region after the overlapping zone), shown in Figure 5d, the change of error between different refinement levels is towards positive values in all grid sets with more pronounced effects on Y_1 and Y_2 probes.

In general, larger errors are seen in each grid set and for X probes further away from the inlet (X_1 to X_4). To a large extent, GS2 and GS3 in all X probes are similar in each refinement level showing better interpolations between the overset and the background regions for the restrained overset. The errors in Y_3 (and respectively Y_4)

in GS4, GS3 and to some extent also GS2 for each specific X probe are almost similar, which imply that the results are affected less from the refinements related to the overset region. The errors of $n = 2, 1.5$, and to some extent $n = 1$, in X_4 and GS1 in all Y probes are larger than those of X_3, possibly because the error moves towards positive values from X_1 to X_3, hence in X_3 the error magnitude becomes smaller and then for X_4 the errors are become positive. On the other hand, for $n = 0.5$ the error increases in negative values. It should be mentioned that no significant wave encounter period change is seen in the wave propagation simulations and it remains below 0.2% of the wave encounter period. More observations could be discussed in future including the analysis of the 2^{nd} harmonic amplitudes.

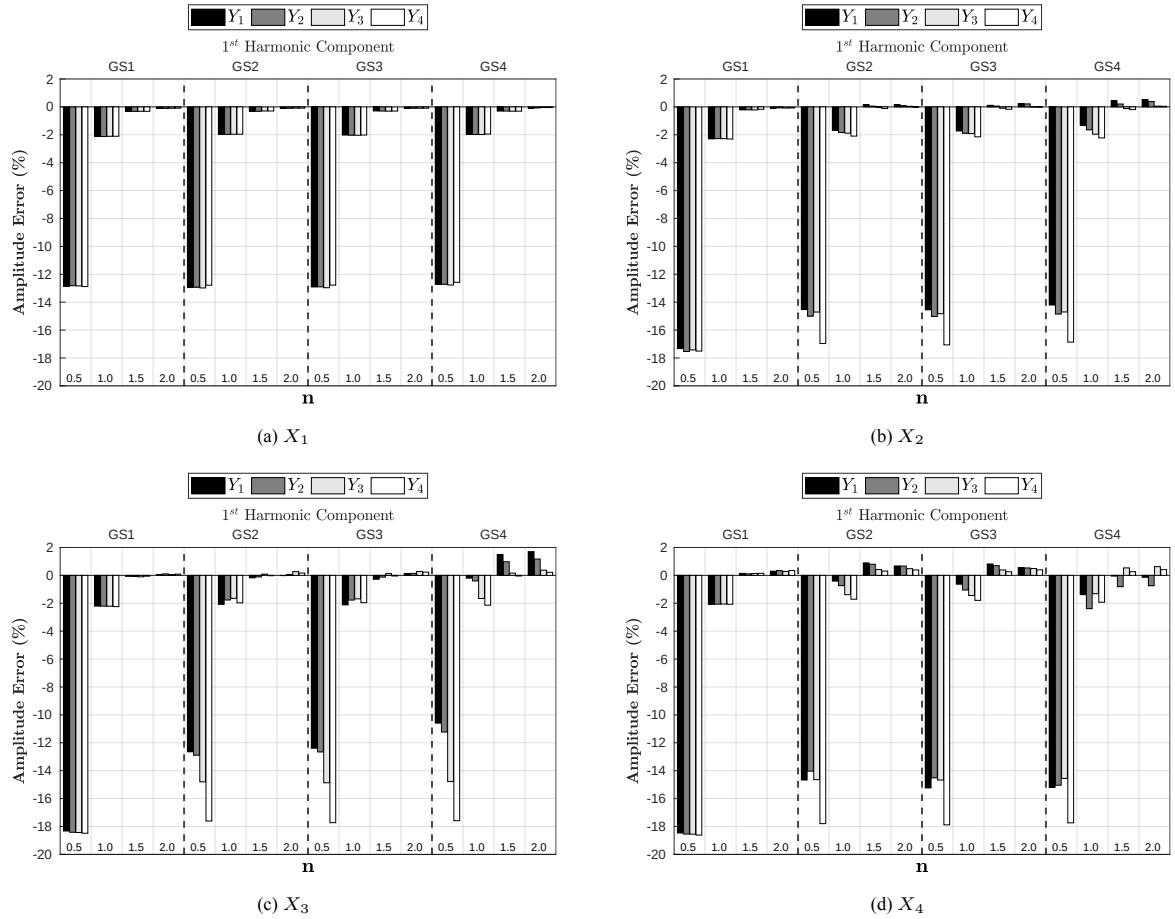

(a) X_1 (b) X_2

(c) X_3 (d) X_4

Figure 5: The Fourier analysis results of the wave elevation at the probes for turbulent flow simulations in SW-3D.

The Fourier analysis is carried out for the hull performance simulations in GS5 for 6 encountered wave periods after convergence (under discussion) in each refinement level. The numerical uncertainty analysis of the grids is carried out by a method proposed in [5]. The mean (0^{th} harmonic amplitude) of resistance (for a half hull) and the first harmonic amplitudes of heave and pitch motions for different refinement ratios, are presented in Figure 6. The mean value of the heave and pitch motions are very small (close to the calm water sinkage and trim), therefore, the incorporated uncertainties of such parameters would become unjustifiably large and therefore not presented here.

The numerical uncertainty of mean resistance for the finest grid ($n = 2$) is close to 16% and the highest uncertainty is seen for $n = 1.0$. The resistance values computed in all grids are relatively similar which are close to the experimental value. The uncertainty of the 1^{st} harmonic amplitude of heave motion is similar in all grids and the heave motion exhibits a stable trend in all grids even though the magnitude of such parameter is very small. An interesting grid convergence is seen for the pitch 1^{st} harmonic amplitude with largest uncertainty at coarsest grid $n = 0.5$ and smallest at the finest grid $n = 2.0$. The experimental data related to motions are not included in the plots due to very small and rounded values.

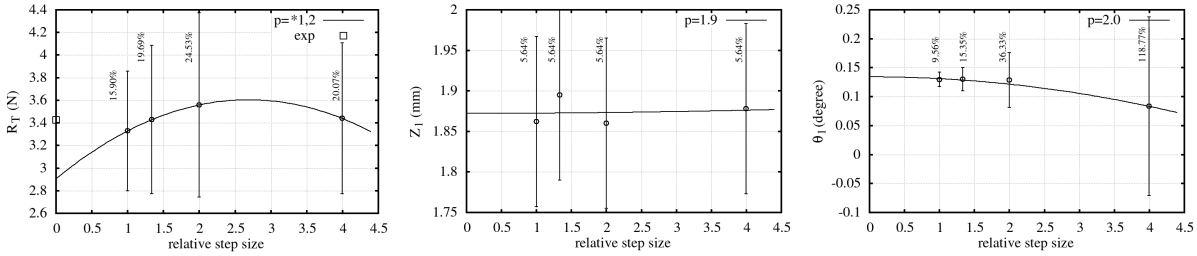

(a) Mean of total resistance. (b) The 1^{st} harmonic amplitude of heave motion. (c) The 1^{st} harmonic amplitude of pitch motion.

Figure 6: The uncertainty analysis of the hull performance in waves in GS5.

Mean of the surface averaged y^+ over the wetted surface area of the hull during one wave encounter period is approximately 208, 102, 66, 49 for $n = 0.5 - 2.0$, respectively. The computational costs per each encountered wave period in terms of core-hours are provided in Figure 7. The computational costs are clearly much higher for the finer grids in each grid set.

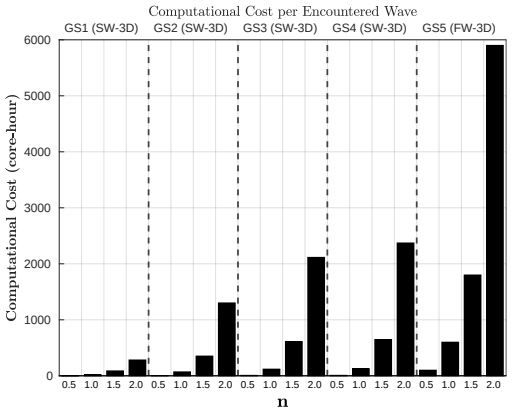

Figure 7: Computational costs per encountered wave period of simulation.

CONCLUDING REMARKS and FUTURE WORK

The numerical uncertainties of the finest grid is about 16%, 6% and 10% for the ship resistance and the first harmonic of heave and pitch motions, respectively. The uncertainties increase for the coarser grids. The computational cost of the finest mesh is several times larger than the other coarser grids which makes it impractical for further investigations with respect to the available computational resources. However, it should be highlighted that the hull motions are very small for $\lambda/L = 0.6$. Therefore, small changes in the final result cause large uncertainties. We expect that the uncertainties decrease for the longer wave lengths where the motions are more dominant. The validity of this hypothesis will be investigated in the continuation of this study.

REFERENCES

[1] P. Roache. Verification of codes and calculations. AIAA Journal, 5:696-702, 36, (1998).

[2] K. Ho. Phase-Averaged SPIV Wake Field Measurement for KVLCC2 Propeller Plane in Waves. PhD Thesis, Osaka University, Japan. (2014)

[3] P. Crepier. Ship Resistance Prediction: Verification and Valication Exercise on Unstructured Grids. MARINE 2017, Wageningen, The Netherlands.

[4] ITTC, 2014. International Towing Tank Conference. Recommended Procedures and Guidelines 7.5-03-02-03, “Practical Guidelines for Ship CFD Applications”, 27^{th} ITTC, 2014.

[5] L. Eça and M. Hoekstra, A procedure for the estimation of the numerical uncertainty of CFD calculations based on grid refinement studies, Journal of Computational Physics, Volume 262, Pages 104-130, doi:10.1016/j.jcp.2014.01.006. (2014)